2-D E-SCATTERING BY A RIGHT ANGLE DIELECTRIC WEDGE

A. G. Tyzhnenko

Department of Mathematics, Kharkov State Economic University,
9-A Lenin Ave. 61059 Kharkov, Ukraine
email: tyzhnenko@ksue.edu.ua

Abstract

A novel numerical method for the right angle dielectric wedge (RADW) boundary value problem (BVP) solving in full wave formulation is presented. This one uses a Sommerfeld-like integral representation of scattered fields inside and outside a wedge and matching these fields on the boundaries. This procedure yields a six-order system of 1st kind integral equations, which is correct in functional meaning only for a cylindrical incident wave. Laplace transform casts this system in equivalent form more suitable for numerical treating. After discretization, one obtains a very ill-conditioned matrix equation (ME). To solve such equations, a new iterative method is proposed.

1. INTRODUCTION

The diffraction of an E-polarized plane wave by a RADW has been treated by a number of authors; see for example [1-5]. The aim of these authors was to obtain an exact closed form solution to the 2-D Fredholm IE of electromagnetics, first obtained in [6]. However, the rigorous solution that is valid for numerical analysis is not available to date. Some approximate solutions are also known. Rawlins [7] obtained a Neumann series solution and calculated the first term in the series, which is valid for small dielectric constants. Berntsen [8] dealt with this problem with the Fredholm IE for unknown surface field and solved it iteratively for limited values of dielectric constants ($\varepsilon < 10$). An asymptotic solution to this problem was obtained in [9]. A scattered far field was built as a geometric-optical field and a cylindrical wave diffracted from the edge. In all mentioned papers, far fields were obtained approximately, but there were no backscattered fields in these works. However, it is important to know the field behavior in the vicinity of the tip of the wedge and backscattered far fields.

One of principal difficulties posed in the problem of a plane wave scattering by a dielectric wedge is, to our opinion, the absence of a simple form of solution inside and outside the wedge because we cannot represent such a solution as a linear combination of plane and cylindrical waves. This situation changes for a cylindrical incident

wave. In this case, we have cylindrical waves only that permits us to use simple integral representations for inside and outside fields and to satisfy the boundary conditions along the whole dielectric interface.

Using a cylindrical incident wave permits us to obtain in presented paper an analytical form of approximate solution and to compute the EM fields at any observation point. An asymptotic approximation of obtained solution gives the far field in any direction.

A canonical method of fields matching on the boundaries is used in this paper. Fields inside and outside the wedge are represented in integral form in the right-angle coordinates. Then, the boundary conditions lead to a set of IE of the 1st kind for six spectral functions. These equations have a continuous integrable solution for a cylindrical incident wave. The Laplace transform of the obtained IE results in an ill-conditioned matrix equation (ME) obtained with the aid of point-matching method. The main problem of solving mentioned boundary-value problem with the aid of such canonical method is to obtain an adequate solution to very ill-conditioned ME resulted from corresponding IE set. An appropriate iterative scheme was proposed in [10, 11] for this purpose, since the known iterative methods do not work for very large condition numbers. However, the iterative algorithm derived in [10, 11] has only a numerical convergence. In this work, we develop a new iterative scheme, which gives a convergent solution practically for any conditioning. This new iterative algorithm has very fast convergence. This prevents usually observable accumulation of rounding errors when solving an ill-conditioned ME.

2. BOUNDARY-VALUE PROBLEM

It is assumed that the dielectric body with a relative permittivity ε occupies the 1st quadrant ($x \geq 0, y \geq 0$). The permittivity of the wedge will be a complex constant value $\varepsilon = \varepsilon' + j\varepsilon''$ with $\varepsilon'' < 0$. Outside the wedge, the relative permittivity is denoted by ε_1. We consider a cylindrical incident wave with only z-component of electric field incoming from a source point ($x_0 = -\rho_0 \sin i_0$, $y_0 = -\rho_0 \cos i_0$).

$$E_0(x, y) = aH_0^{(2)}\left(k_0\sqrt{(x - x_0)^2 + (y - y_0)^2}\right)e^{j\omega t} \tag{1}$$

We assume that ρ_0 is asymptotically large, and i_0 is the incident angle counted clockwise from the negative y-axis. We denote here $k_0 = \omega\sqrt{\varepsilon_1}/c$ and omit henceforth the time dependence. To solve this BVP for the 2-D wave equation, a total electric field inside the wedge (D_1) is represented as the sum of Witteker's integrals:

$$E_1(x,y) = \int_{-\infty}^{\infty} A_1(\xi) e^{-j\xi x - jh y} d\xi / h + \int_{-\infty}^{\infty} A_2(\xi) e^{-jh x - j\xi y} d\xi / h . \tag{2}$$

Outside the wedge we use analogous representation to the scattered field in the 2nd quadrant (D_2):

$$E_2(x,y) = \int_{-\infty}^{\infty} A_3(\xi) e^{jh_0 x - j\xi y} d\xi / h_0 + \int_{-\infty}^{\infty} A_4(\xi) e^{j\xi x - jh_0 y} d\xi / h_0 \tag{3}$$

and in the lower half-space (D_3):

$$E_3(x,y) = \int_{-\infty}^{\infty} A_5(\xi) e^{-j\xi x + jh_0 y} d\xi / h_0 + \int_{-\infty}^{\infty} A_6(\xi) e^{j\xi x + jh_0 y} d\xi / h_0 \tag{4}$$

where $h = \sqrt{k^2 - \xi^2}$, $h_0 = \sqrt{k_0^2 - \xi^2} = -j\sqrt{\xi^2 - k_0^2}$, $k = \omega\sqrt{\varepsilon}/c$. Functions (2-4) satisfy the corresponding wave equations and radiation conditions inside and outside the wedge for arbitrary integrable in R_1 function $A_i(\xi)$. These representations have the meaning of plane wave decompositions and must account for all waves of a physical problem. It is clear that it is so for a right angle wedge. The boundary conditions for the electric and magnetic fields are the following:

$$E_1(x,0) - E_3(x,0) = E_0(x,0) \tag{5a}$$

$$\frac{\partial}{\partial y} E_1(x,0) - \frac{\partial}{\partial y} E_3(x,0) = \frac{\partial}{\partial y} E_0(x,0), \qquad x \ge 0 \tag{5b}$$

$$E_1(0,y) - E_2(0,y) = E_0(0,y) \tag{5c}$$

$$\frac{\partial}{\partial x} E_1(0,y) - \frac{\partial}{\partial x} E_2(0,y) = \frac{\partial}{\partial x} E_0(0,y), \qquad y \ge 0 \tag{5d}$$

$$E_2(x,0) - E_3(x,0) = 0 \tag{5e}$$

$$\frac{\partial}{\partial y} E_2(x,0) - \frac{\partial}{\partial y} E_3(x,0) = 0 \ , \qquad x \le 0 \tag{5f}$$

If Eqs. (1), and (2-4) are substituted into Eqs. (5), we obtain the set of six IE of the first kind. It is important to clear up a solvability of this system. The equation (5) may be considered as the Fourier representation of the right-hand side (RHS). Such a representation exists if the RHS tends to zero at infinity. This condition is true for a cylindrical incident wave. As the Hankel function (1) oscillates with the wave number k_0 and its amplitude decreases monotonously to zero at infinity, its Fourier spectral function has only two points of discontinuity at $\xi = \pm k_0$. At other points its spectral function is continuous [12]. These two singular points are accounted for in the field representation (2-4) that permits us to find the unknown functions $A_i(\xi)$ in the class of integrable continuous functions C_{L_1}. To find the solution in the whole space, we apply the Laplace transformation to the set (5) and obtain the equivalent new set:

$$\int_{-\infty}^{\infty} A_1 \frac{d\xi / h}{\nu - \xi} + \int_{-\infty}^{\infty} A_2 \frac{d\xi / h}{\nu - h} - \int_{-\infty}^{\infty} A_5 \frac{d\xi / h_0}{\nu - \xi} - \int_{-\infty}^{\infty} A_6 \frac{d\xi / h_0}{\nu + \xi} = \frac{b}{\nu - k_0 \sin i_0} \tag{6a}$$

$$\int_{-\infty}^{\infty} A_1 \frac{d\xi / h}{\nu - h} + \int_{-\infty}^{\infty} A_2 \frac{d\xi / h}{\nu - \xi} - \int_{-\infty}^{\infty} A_3 \frac{d\xi / h_0}{\nu - \xi} - \int_{-\infty}^{\infty} A_4 \frac{d\xi / h_0}{\nu - h_0} = \frac{b}{\nu - k_0 \cos i_0} \tag{6b}$$

$$\int_{-\infty}^{\infty} A_1 \frac{\xi\, d\xi / h}{\nu - h} + \int_{-\infty}^{\infty} A_2 \frac{d\xi}{\nu - \xi} + \int_{-\infty}^{\infty} A_3 \frac{d\xi}{\nu - \xi} + \int_{-\infty}^{\infty} A_4 \frac{\xi\, d\xi / h_0}{\nu - h_0} = \frac{b k_0 \sin i_0}{\nu - k_0 \cos i_0} \tag{6c}$$

$$\int_{-\infty}^{\infty} A_3 \frac{d\xi / h_0}{\nu - h_0} + \int_{-\infty}^{\infty} A_4 \frac{d\xi / h_0}{\nu - \xi} - \int_{-\infty}^{\infty} A_5 \frac{d\xi / h_0}{\nu + \xi} - \int_{-\infty}^{\infty} A_6 \frac{d\xi / h_0}{\nu - \xi} = 0 \tag{6d}$$

$$\int_{-\infty}^{\infty} A_1 \frac{d\xi}{\nu - \xi} + \int_{-\infty}^{\infty} A_2 \frac{\xi\, d\xi / h}{\nu - h} + \int_{-\infty}^{\infty} A_5 \frac{d\xi}{\nu - \xi} + \int_{-\infty}^{\infty} A_6 \frac{d\xi}{\nu + \xi} = \frac{b k_0 \cos i_0}{\nu - k_0 \sin i_0} \tag{6e}$$

$$\int_{-\infty}^{\infty} A_3 \frac{\xi\, d\xi / h_0}{\nu - h_0} + \int_{-\infty}^{\infty} A_4 \frac{d\xi}{\nu - \xi} + \int_{-\infty}^{\infty} A_5 \frac{d\xi}{\nu + \xi} + \int_{-\infty}^{\infty} A_6 \frac{d\xi}{\nu - \xi} = 0 \,. \tag{6f}$$

This set is solved with the aid of collocation method using quadratures formulae while performing discretization. We denote here $\nu = \nu' + j\sigma, \nu' \in R_1$ and

$$b = a\sqrt{\frac{2}{\pi}} \frac{\exp(jk_0\rho_0 + j\pi/4)}{\sqrt{k_0\rho_0}} \,.$$

The Laplace transformations to the Hankel functions in the RHS of (5) are derived asymptotically by assuming that $\rho_0 \to \infty$ and using the stationary–phase method. We henceforth put $|b|=1$ for brevity.

The set (6) is more suitable for numerical solution because of having a square integrable RHS. Hence, the corresponding matrix equation which is obtained while discretization also has a square summable RHS that is necessary for an existing solution in the infinite-dimensional vector space l_1 with 1-norm

$$\| A \|_1 = \sum_{i=1}^{\infty} | A_i | < \infty . \tag{7}$$

The obtained ME has a very ill-conditioned matrix. Its condition number is about 10^{19}. Because of very large condition number of the main matrix, the known iterative techniques, such as gradient methods, do not work in this case. Therefore, a new iterative scheme developed by the author in [10, 11] for such systems solving. In this work, in contrast to the previous work [11], we propose a convergent and very fast iterative algorithm, which permits one to avoid practically the undesirable accumulation of rounding errors when solving very ill-conditioned MEs.

3. ITERATIVE TECHNIQUE

Consider a common ME

$$Kx = f \tag{8}$$

where K is a square nonsingular matrix of m-th order, x and f are vectors. Let consider further the equivalent equation

$$K^* Kx = u \tag{9}$$

where K^* is the Hermitian adjoint matrix and $u = K^* f$. One can transform this equation to the iterative form adding αx on both sides as

$$(\alpha I + K^* K)x = u + \alpha x \tag{10}$$

with $\alpha > 0$ and I being the m-th order identity matrix. Let denote the i-th eigenvalue of K as $\lambda_i(K)$ and corresponding singular number as

$$\sigma_i(K) = \sqrt{\lambda_i(K^* K)} \equiv \sigma_i \,. \tag{11}$$

Accounting for $\lambda_i(K^* K + \alpha I) = \sigma_i^2 + \alpha > 0$, one can see that the matrix $K^* K + \alpha I$ has a unique inverse one, viz., $(K^* K + \alpha I)^{-1}$, which permits one to re-write the equation (10) in the iterative form

$$x = b + Gx \tag{12}$$

where $b = (K^* K + \alpha I)^{-1} u$ and

$$G = \alpha (K^* K + \alpha I)^{-1} . \tag{13}$$

To the equation (12) corresponds the simple iterative scheme

$$x_n = b + G x_{n-1} \tag{14}$$

which converges if and only if the spectral radius $\rho(G)$ of the matrix *G* is less than 1, namely,

$$\rho(G) = \max_i |\lambda_i(G)| < 1 . \tag{15}$$

Accounting for $\rho(G) \le \| G \|$ with $\| \cdot \|$ being a spectral norm, let prove that $\| G \| < 1$ for any $\alpha > 0$. Really, let account for $\| G \| = \alpha \| (K^* K + \alpha I)^{-1} \|$ and that the spectral norm of a matrix equals to its maximum singular value. Then,

$$\| G \| = \alpha \max_i \sigma_i((K^* K + \alpha I)^{-1}) . \tag{16}$$

Noting $D = K^* K + \alpha I$ and accounting for $D^* D = D^2$, one can derive that $\sigma_i^2(D) = \sigma_i^2 + \alpha$ and then,

$$\| G \| = \frac{\alpha}{\min_i \sigma_i^2 + \alpha} \tag{17}$$

if using the known relation $\sigma_i(D^{-1}) = 1/\sigma_i(D)$. Because of $\min_i \sigma_i^2 > 0$ for nonsingular matrix *K*, we obtain from (17) that $\| G \| < 1$ and hence the iterative algorithm (14) converges. In this case, the approximate solution x_n tends to an exact solution of equation (12), which can be represented as

$$x = \sum_{n=0}^{\infty} G^n b = K^{-1} f \tag{18}$$

with the inverse matrix

$$K^{-1} = \sum_{n=0}^{\infty} G^n (K^* K + \alpha I) K^* \tag{19}$$

Considering K^{-1} as a matrix operator in a finite linear space, we can easily see that it is continuous and hence, the solution x (18) is stable in the sense of Hadamard.

There are many iterative algorithms derived to now. All these differ only by a total computational labor for well-conditioned ME. However, for ill-conditioned ME the convergence rate decreases and needed accuracy is achieved for greater iteration number N. This issue leads to accumulation of rounding errors as was noted in [13]. As a result, a theoretically convergent iterative solution can tend to some other solution. This issue depends only on the number (N) of needed iterations and the latter depends on the rate of convergence and may lead to an inadequate solution in the case of ill-posedness. The adequacy of an iterative solution to verify, one can check the validity of approximate inverse matrix

$$K_N^{-1} = \sum_{n=0}^{N} G^n (K^* K + \alpha I) K^* \tag{20}$$

obtained as a result of N iterations. The inadequacy error can be then estimated as

$$e_N = \| K_N K_N^{-1} \| - 1 \tag{21}$$

For very ill-conditioned ME with condition number $\sim 10^{19}$ there exists an optimal iterations number N_{opt} which minimizes the error (21). Practically, an iterative solution can be regarded as adequate if the error (21) is less than 10^{-3} and relative residual error of an ME solution is of the same order or less. All numerical results obtained in this paper when solving the RADW BVP problem are in the range of such accuracy.

It is worthwhile to point out that proposed iterative algorithm is drastically faster than that of derived in [11]. The new method achieved mentioned accuracy by approximately 10 iterations in contrast to about 1000 in [11]. Such a convergence rate prevents primarily the accumulation of rounding errors and permits one to obtain es-

sentially adequate solution to any ill-conditioned ME, which is good arranged. The last issue is related with preconditioning procedure and determines the existence of a solution. In this paper, we use the Laplace transform of the integral equations in (5) as a preconditioning procedure.

4. NUMERICAL RESULTS

A collocation method was used in this paper for the IE set (6) for solving in the class of continuous integrable functions with the aid of discretization by the quadratures. The integration range was reduced to a finite one due to the physical considerations that permit us to assume that the spectral functions $A_i(\xi)$ are concentrated not far from geometric-optical points and numerical investigations prove that. In Fig. 1 the 1st (from six) solution is shown for $\varepsilon = 10$ and incidence angle $i_0 = 45^\circ$. We can see here the integrability of the solution and its independence of the integration range. We put k_0=1 and use the same meshing for ξ and ν'. The range $\xi, \nu' \in [-8, 8]$ was used during integration in Eqs. (6), for dielectric constant less than 60. The interval $\xi \in [-1, 1]$ was sampled at 0.1051 and the rest of the range was sampled at 0.3684. Enlarging the integration range up to [-20, 20] was tested and the solution did not change. For permittivity greater then 60 the integration range must be enlarged. Parameter σ in (6) was varied in the range 0.5 – 0.9, to find a minimal discrepancy. The mentioned discretization produces the matrix K of the size 462×462 with the condition number about of 10^{19}. The CPU time to the ME solving with the aid of iterative scheme (14), having tolerance level equals to 10^{-3}, was about 30 sec on a PC Pentium Pro 200 MHz (with the code written in MATLAB). For the mentioned parameters, the boundary condition matching relative error in the vicinity of the edge was less then 0.5%.

The spectral functions $A_{1,2}(\xi)$ determine the total field inside the wedge using Eq. (2). Functions $A_{3,4}(\xi)$ and $A_{5,6}(\xi)$ determine the scattered field in the 2nd quadrant and in the lower half-space, if using Eqs. (3 and 4), respectively. The far field was evaluated asymptotically from Eqs. (2-4) according to [14]:

$$E(\rho, \vartheta) = F(\vartheta) e^{-jk_0 n\rho} / \sqrt{k_0 \rho} \tag{22}$$

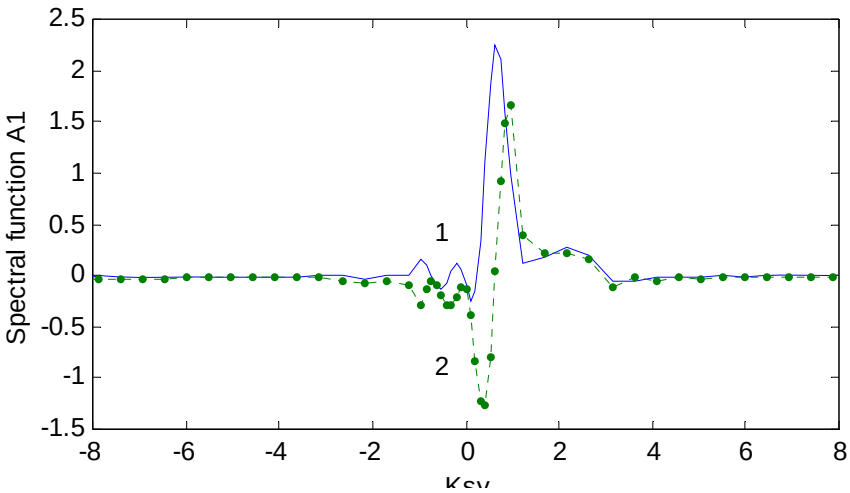

Figure 1. Typical solution of the BVP. Real and imaginary part of the first (from six) spectral function $A_1(\xi)$ for ε=10 and $i_0 = 45^\circ$.

with

$$F(\vartheta) = \sqrt{\frac{2\pi}{n}}\, e^{j\pi/4} \begin{cases} A_1(k_0 n\cos\vartheta) + A_2(k_0 n\sin\vartheta), & 0^\circ \le \vartheta \le 90^\circ, \quad n = \sqrt{\varepsilon} \\ A_3(k_0 n\sin\vartheta) + A_4(-k_0 n\cos\vartheta), & 90^\circ \le \vartheta \le 180^\circ, n = 1 \\ A_5(k_0 n\cos\vartheta) + A_6(-k_0 n\cos\vartheta), & -180^\circ \le \vartheta \le 0^\circ, n = 1 \end{cases}$$

for the total field inside the wedge ($0^\circ \le \vartheta \le 90^\circ$) and for the scattered fields in the 2nd quadrant and in the lower half-space . The far-field amplitude patterns $|F(\vartheta)|$ are shown in Fig. 2 for the nose illumination ($i_0 = 45^\circ$) and for various permittivities. Here we can see the focusing effect of Rawlins [7] in Fig. 2(a) for small dielectric constants (ε=1.5, 2). This effect vanishes rapidly with permittivity growth and the total field concentrates near verges for ε=50 (curve 6). The scattering in the lower half-space for the same cases is shown in Fig. 2(b). We can see here the main maximum approximately in geometric-optical direction and backscattered field maximum ($\vartheta \approx -135^\circ$) for each pattern. Some asymmetry that we can see here is caused by the lack of accuracy.

For the negative incidence angle ($i_0 \le 0$) we use another field representation in the 2nd quadrant. In this case $E_2(x, y)$ in Eq. (3) will be a total field.

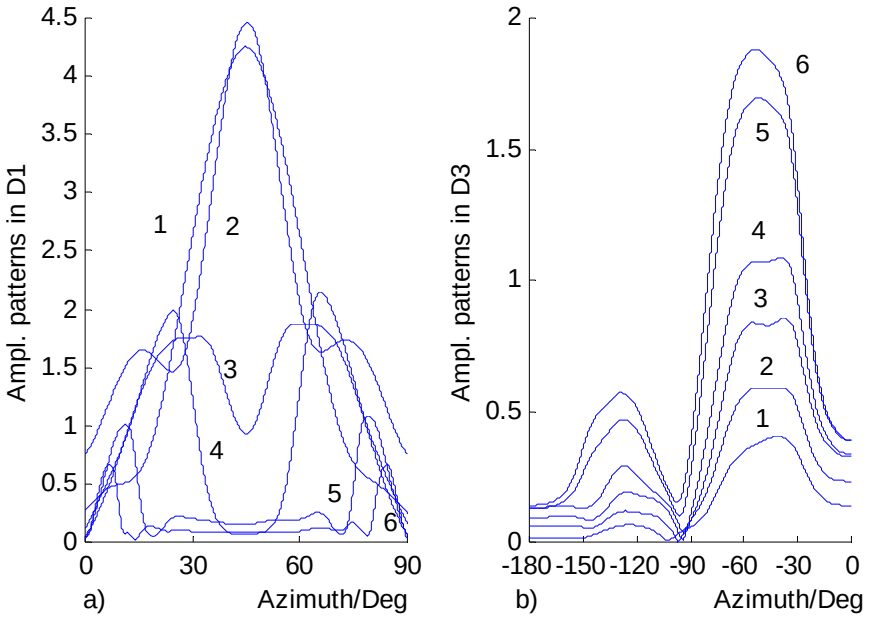

Figure 2 (a) Total far-field patterns inside the wedge for nose illumination ($i_0 = 45^\circ$) and ε=1.5, 2, 3, 5, 20, 50 (curves 1-6). (b) Scattered far-field patterns in the lower half-space for the same parameters.

The scattered far-field patterns for ε=50 and oblique incidence ($i_0 = -85^\circ$, curve 1, and $i_0 = -70^\circ$, curve 2) are compared in Fig. 3 with frontal incidence pattern ($i_0 = 0^\circ$, curve 3). We see approximately the same patterns for $i_0 = -85^\circ$ and $i_0 = -70^\circ$ with two symmetric maxima ($\vartheta \approx \pm 145^\circ$) in the forward direction, one maximum ($\vartheta \approx -90^\circ$) for the side scattering, and one maximum ($\vartheta \approx -45^\circ$) in the back direction. When increasing i_0 to zero the main maximum occur at $\vartheta \approx -90^\circ$ (the backscattering) as is shown in Fig. 3(a), curve 3. In the 2nd quadrant we can see in Fig. 3(b) the total field increasing for $i_0 = 0^\circ$ (curve 3) in the forward direction, as it must be from general considerations.

The backscattering estimation that becomes possible due to the proposed method using gives the opportunity to calculate the dimensionless monostatic RCS (MRCS) according to formulae

$$\sigma = \lim_{\rho \to \infty} 2\pi k_0 \rho |E_s|^2 / |E_0(0,0)|^2 \tag{20}$$

for the nose illumination of the wedge ($i_0 = 45^\circ$) with the incident wave normalization: $|E_0(0,0)| = 1$. In this case, the backscattered field is the field scattered by the

edge only. It is important to investigate the backscattering from the edge for some real absorbers.

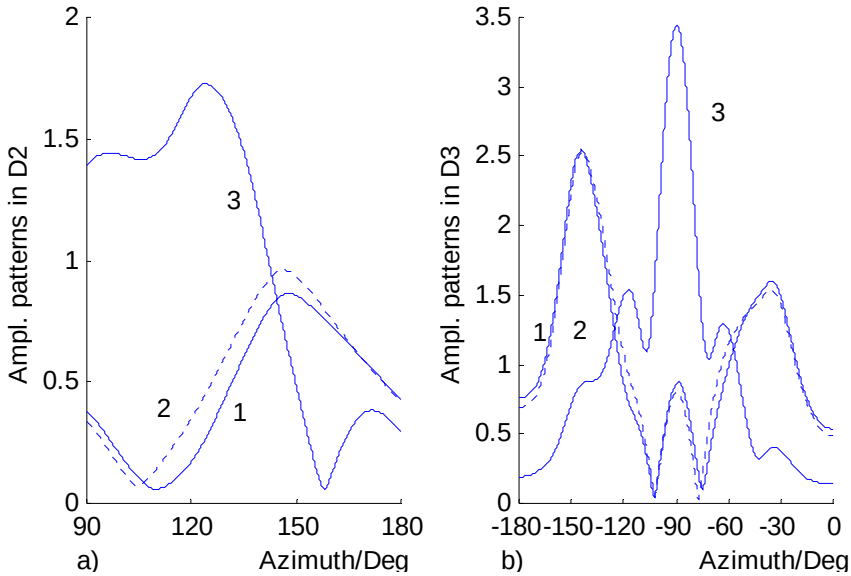

Figure 3. (a) Total far-field patterns in the 2nd quadrant for negative incident angles ($i_0 = -85^\circ$, curve 1, and $i_0 = -70^\circ$, curve 2) compared with the normal incidence ($i_0 = 0^\circ$, curve 3) for ε =50. (b) Scattered far-field patterns in the lower half-space for the same parameters.

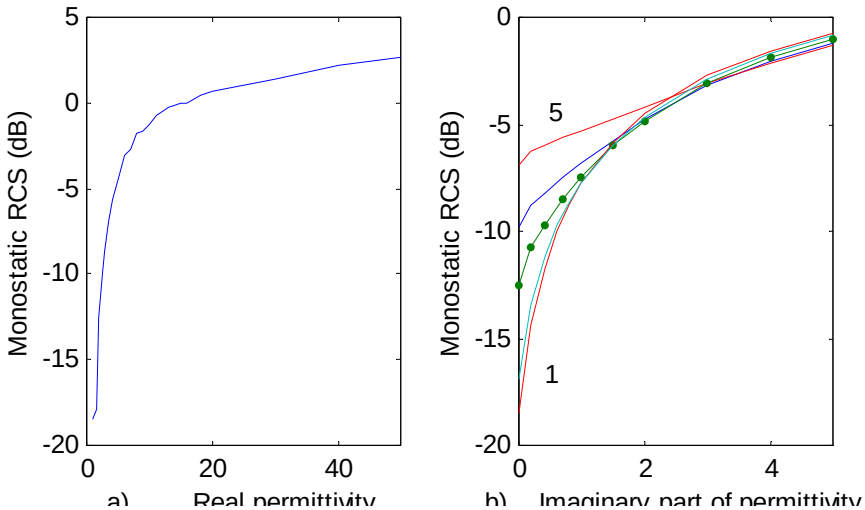

Figure 4. (a) MRCS via real permittivity value for nose illumination ($i_0 = 45^\circ$). (b) MRCS via imaginary part of permittivity for some absorbers with ε =1.4, 1.6, 2, 2.5, 3.45 (curves 1-5).

Fig. 4(a) shows the MRCS dependence via real permittivity in the range of 1.4-50. Fig. 4(b) shows the analogous dependence of MRCS via imaginary part of permittivity (ε'') for some absorbers (ε=1.4, 1.6, 2, 2.5, 3.45). With the aid of such calculations we can estimate the effectiveness of a wedge-like covering.

5. CONCLUSION

A full-wave rigorous numerical method to a RADW BVP solving in integral formulation is presented in this paper. The unknown spectral functions $A_i(\xi)$ are obtained approximately as a solution of the 1st kind IE set in the C_{L_1} function class. The point-matching method is used for discretization this IE set, which yields very ill-conditioned ME. A new convergent iterative method is proposed to obtain a unique normal solution for such a ME that is stable in the sense of Hadamard and immune to the sampling variations. The obtained solution ensures the boundary conditions matching error less than 0.5% in the vicinity of the edge. The analytical form (2-4) of the BVP solution permits to compute fields and their derivatives at any point without complicated calculations. The far-field amplitude patterns are presented and an essential difference is shown compared with the geometric-optical approximation. The focusing effect of Rawlins is confirmed and backscattered far fields are estimated for small and large permittivities.

REFERENCES

[1] J. Radlow, ”Diffraction by a Right Angled Dielectric Wedge”, Intern. J. Eng. Sc., vol. 2, pp. 275-290, 1964.

[2] V. I. Kurilko, “Scattering of Electromagnetic Waves by a Right Angled Dielectric Wedge”, Izv. V.U.Z. Radiofiz., vol. 9, p.980, 1966.

[3] N.-H. Kuo and M. A. Plonus, “A Systematic Technique in the Solution of Diffraction by a Right Angled Dielectric Wedge”, J. Math. Phys., vol. 46, No. 4, pp. 394-407, 1967.

[4] N. Latz, “Electromagnetic Diffraction by Imperfectly Dielectric Wedges”, J. Math. Anal. Appl., vol. 43, No. 2, pp. 373-387, 1973.

[5] A. A. Aleksandrova and N. A. Khizhnjak, “Diffraction of Electromagnetic Waves by a Dielectric Wedge”, Sov. Phys. Tech. Phys., vol. 44, No. 11, pp. 2241-2249, 1974.

[6] N. A. Khizhnjak, “The Green’s Function for the Maxwell’s Equations”, Sov. Phys. Tech. Phys.,vol. 28, No. 7, pp. 1592-1609, 1958.

[7] A. D. Rawlins, “Diffraction by a Dielectric Wedge”, J. Inst. Math. Applics., Vol. 19, No. 3, pp. 261-279, 1977.

[8] S. Berntsen, “Diffraction of an Electric Polarized Wave by a Dielectric Wedge”, SIAM J. Appl. Math., vol. 43, No. 1, pp. 186-211, 1983.

[9] C.-S. Joo, J.-W. Ra and S.-Y. Shin, “Scattering by Right Angle Dielectric Wedge”, IEEE Trans. Antennas Propagat., vol. AP-32, No. 1, pp. 61-69, 1984.

[10] A. G. Tyzhnenko, “Low-Grazing-Angle Scattering by a Triangle Model of an Ocean Wave”, Proc. Int. Conf. Mathematical Methods in EM Theory (MMET*2000), Kharkov, pp. 417-419, 2000.

[11] A. G. Tyzhnenko, “Cylindrical E-Wave Scattering by a Right Angle Dielectric Wedge”, Electromagnetics, Vol. 22, No. 6, pp. 487-498, 2002.

[12] S. Bochner, “Lectures on Fourier Integrals”, Princeton, NJ, Princeton University Press, p. 25, 1959.

[13] N. S. Bachvalov, N. P. Jydkov, G. M. Kobelkov, “Numerical methods”, Moscow, “Nauka”, 1987 (in Russian).

[14] L. B. Felsen and N. Markuvitz, “Radiation and Scattering of Waves”, Prentice-Hall, Inc., Englewood Cliffs, N. J., 1973.